Journal of Cardiovascular Magnetic Resonance (2007) **9,** 49–56

ISSN: 1097-6647 print / 1532-429X online
DOI: 10.1080/10976640600897427

Reproducibility of Free-Breathing Cardiovascular Magnetic Resonance Coronary Angiography

Gerald F. Greil, MD,[1,*] Milind Y. Desai, MD,[2,4,*] Michael Fenchel, MD,[3] Stephan Miller, MD,[3] Roderic I Pettigrew, MD PhD,[2] Ludger Sieverding, MD,[1] and Matthias Stuber, PhD[4]

Department of Pediatric Cardiology, University of Tuebingen, Tuebingen, Germany[1], National Institutes of Health, Bethesda, Maryland, USA[2] Department of Radiology, University of Tuebingen, Tuebingen, Germany[3], Russell. H. Morgan Department of Radiology and Radiologic Sciences, Johns Hopkins University, Baltimore, Maryland, USA[4]

ABSTRACT

***Objective*: Contemporary free-breathing non contrast enhanced cardiovascular magnetic resonance angiography (CMRA) was qualitatively and quantitatively evaluated to ascertain the reproducibility of the method for coronary artery luminal dimension measurements. *Subjects and Methods*: Twenty-two healthy volunteers (mean age 32 ± 7 years, 12 males) without coronary artery disease were imaged at 2 centers (1 each in Europe and North America) using navigator-gated and corrected SSFP CMRA on a commercial whole body 1.5T System. Repeat images of right (RCA, n = 21), left anterior descending (LAD, n = 14) and left circumflex (LCX, n = 14) coronary arteries were obtained in separate sessions using identical scan protocol and imaging parameters. True visible vessel length, signal-to-noise (SNR), contrast-to-noise ratios (CNR) and the average luminal diameter over the first 4 cm of the vessel were measured. Intra-observer, inter-observer and inter-scan reproducibility of coronary artery luminal diameter were determined using Pearson's correlation, Bland-Altman analysis and intraclass correlation coefficients (ICC). *Results*: CNR, SNR and the mean length of the RCA, LAD and LCX imaged for original and repeat scans were not significantly different (all p > 0.30). There was a high degree of intra-observer, inter-observer and inter-scan agreements for RCA, LAD and LCX luminal diameter respectively on Bland-Altman and ICC analysis (ICC's for RCA: 0.98. 0.98 and 0.86; LAD: 0.89, 0.89 and 0.63; LCX: 0.95, 0.94 and 0.79). *Conclusion*: In a 2-center study, we demonstrate that free-breathing 3D SSFP CMRA can visualize long continuous segments of coronary vessels with highly reproducible measurements of luminal diameter.**

Keywords: Cardiovascular Magnetic Resonance, Steady State Free Precession, Coronary Artery Imaging, Reproducibility.
[*] The first two authors contributed equally to the work.
We thank EHLKE Foundation, Stiftung zur Förderung der Erforschung von Zivilisationserkrankungen, Baden-Baden, Germany, and Biomedical Engineering Grant from the Whitaker Foundation (RG-02-0745).
M. Stuber, PhD, is compensated as a consultant by Philips Medical Systems NL, the manufacturer of equipment described in this presentation. The terms of this arrangement have been approved by the Johns Hopkins University in accordance with its conflict of interest policies.
Correspondence to:
Matthias Stuber, PhD
Associate Professor
Russell. H. Morgan Department of Radiology and Radiologic Sciences,
Johns Hopkins University,
601 North Caroline Street, JHOC 4243
Baltimore, MD, 21287
tel: 443-287-5241;
fax: 410-614-1977
email: mstuber1@jhu.edu

INTRODUCTION

Atherosclerosis remains the leading cause of death in industrialized societies, and its incidence is projected to increase in the next two decades (1). Coronary artery disease (CAD) accounts for the vast majority of morbidity and mortality associated with atherosclerosis. Traditionally, x-ray angiography is the mainstay for diagnosis of CAD. However, it is an invasive procedure, requiring x-ray exposure and nephrotoxic contrast agents, all of which are associated with a small but significant risk of complications and side-effects. Hence, during the past few years, for the non-invasive assessment of CAD, techniques using cardiovascular magnetic resonance (CMR) and multi-detector computed tomography (MDCT) have been implemented.

CMR, because of its true non-invasive nature, has been successfully applied to visualize proximal and middle portions of the native coronary arteries in individuals with and without CAD (2–5). In a multi-center study, a high degree of sensitivity in detection of significant proximal disease by cardiovascular magnetic resonance angiography (CMRA), compared to conventional x-ray angiography, was demonstrated (2). In order to visualize the coronary tree with a high degree of contrast, multiple different techniques have been utilized. These include the use of fat saturation prepulses (6), T2 preparatory pulses (3,7), implementation of steady state free precession (SSFP) techniques (8) and use of intravascular contrast agents (9–11). Further improvements in respiratory motion correction using navigator technology (12) and electrocardiographic (ECG) gating using vector ECG triggering (13) allow free-breathing high-resolution CMRA with effective suppression of motion artifacts. Hence, as a non-invasive and radiation-free technique, CMRA might be particulary useful for follow-up studies to define different stages of CAD and to assess response to different therapies.

It is feasible to image coronary arteries using a fat-suppressed non-contrast SSFP sequence and furthermore, it leads to an improved SNR and CNR as compared to the older sequences (8). However, to our knowledge, there are no studies demonstrating the reproducibility of three dimensional (3D) free-breathing non-contrast SSFP CMRA. Therefore, the purpose of this study was to qualitatively and quantitatively evaluate the contemporary free-breathing CMRA and to ascertain the reproducibility of the method for coronary artery luminal dimension measurements.

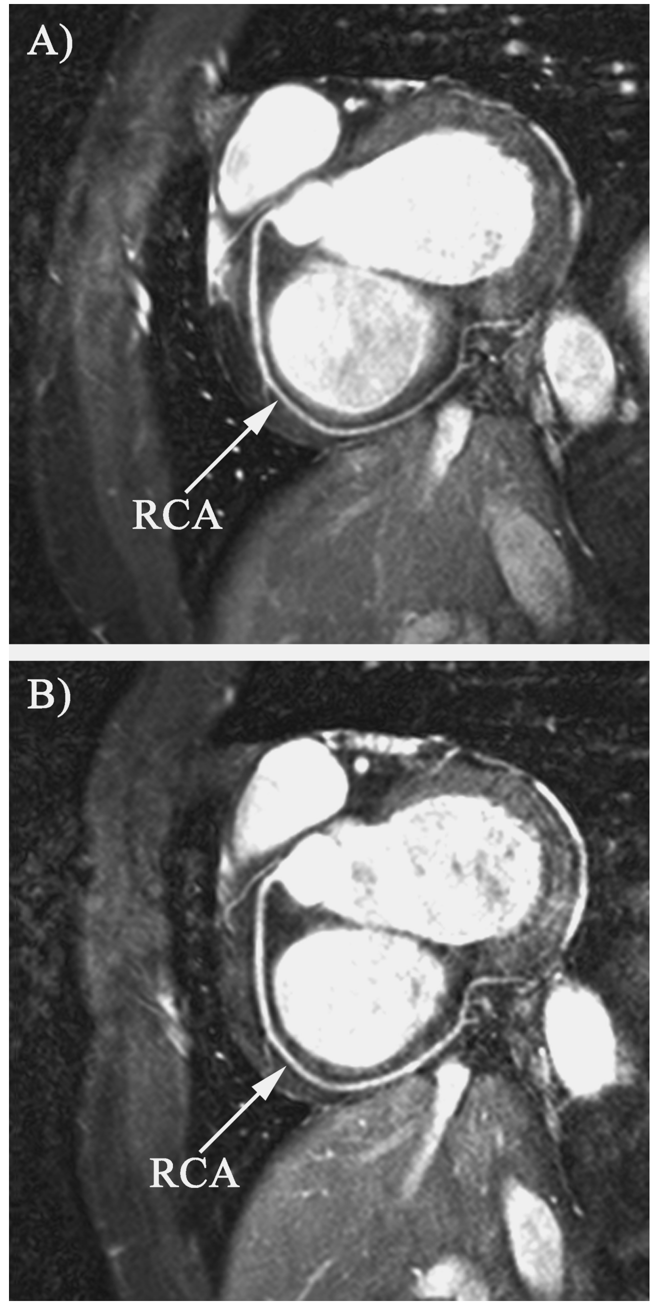

Figure 1. High spatial resolution double oblique navigator-gated and corrected and vector ECG triggered 3D SSFP cardiovascular magnetic resonance angiography of the right coronary artery (RCA) with a T2 preparation pulse for endogenous contrast enhancement obtained during two separate MR sessions (A and B). RCA data were mulitplanar reformatted.

SUBJECTS AND METHODS

This study was conducted at two institutions (one each in Europe and North America) after obtaining appropriate institutional review board approval and HIPAA-compliant informed consent (for North American subjects) from each participant. We consecutively enrolled 22 healthy adult volunteers (mean age 32 ± 7 years, 12 men) without known CAD. All volunteers were in sinus rhythm, without contraindications to CMR. The right coronary artery (RCA) was imaged in 21 volunteers (Fig. 1); both the left anterior descending (LAD) and left circumflex (LCX) (Fig. 2) were imaged in 14 volunteers. The studies and measurements were repeated approximately 1–2 months apart using identical scan protocols and imaging parameters to assess for reproducibility of coronary arterial luminal dimensions, along with comparing the true visible vessel length, signal-to-noise and contrast-to-noise ratios (SNR and CNR) and vessel edge sharpness betweeen the original and repeat studies.

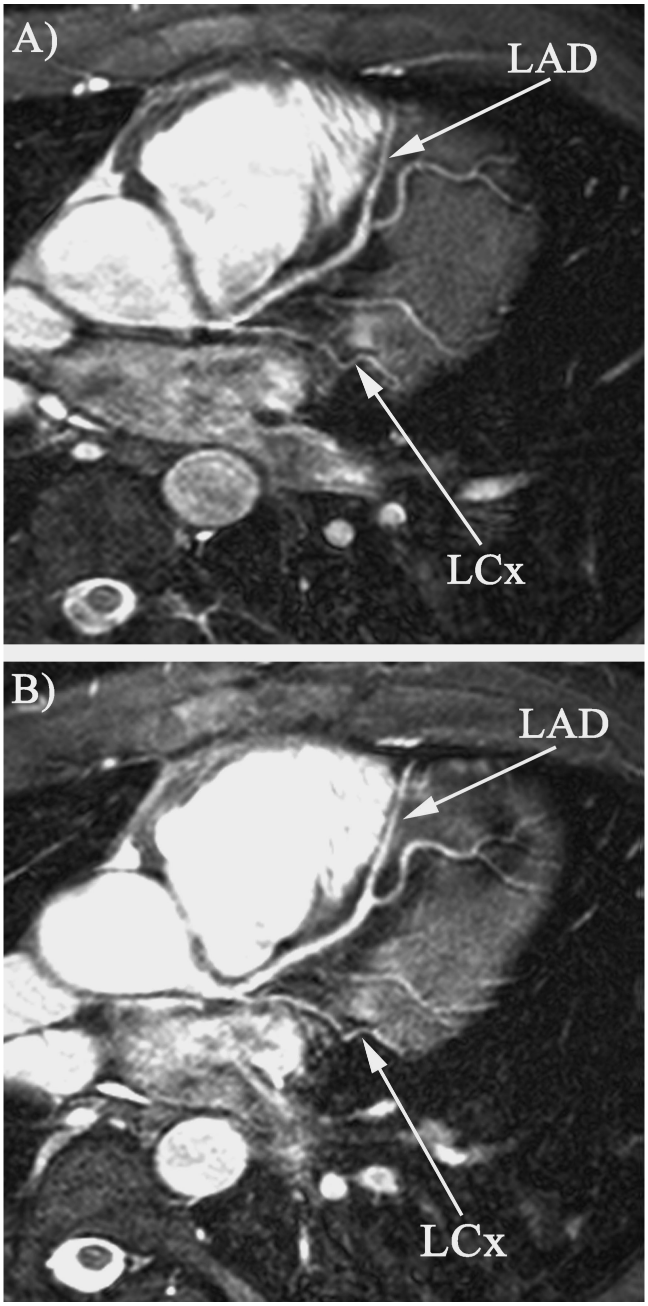

Figure 2. High spatial resolution double oblique navigator-gated and corrected and vector ECG triggered 3D SSFP cardiovascular magnetic resonance angiography of the left coronay artery system with a T2 preparation pulse for endogenous contrast enhancement obtained during two separate MR sessions (**a** and **b**). The left anterior descending (LAD) and left circumflex (LCX) were mulitplanar reformatted.

CMR technique

All studies were performed on a commercial whole body 1.5 T system (Philips Medical Systems, Best, The Netherlands) equipped with cardiac software and a Powertrak 6000 gradient system (gradient strength 23 mT/m, rise time 220 μs). A 5 element phased array cardiac synergy coil (two anterior and three posterior elements) was used for signal reception. All subjects were examined in the supine position, with 4 electrocardiographic leads on the anterior left hemithorax for vector ECG triggering (13). No intravenous contrast agents were used.

Scout imaging

Two scout scans were acquired for coronary artery localization and navigator positioning at the dome of the right hemidiaphragm. The first scout scan was obtained using an electrocardiographically triggered, multisection, two dimensional steady state free precession (SSFP) sequence (TR = 2.21 ms, TE = 0.87 ms, Flip angle = 50°, 10 mm section thickness, 20 coronal, 20 sagittal, 20 axial slices, acquisition time 10 seconds). From the coronal and transverse images of this first scout, the navigator was localized at the dome of the right hemidiaphragm in the foot-head direction for respiratory motion suppression.

Subsequently, a 3D free-breathing navigator gated (5 mm gating window) and corrected low-resolution 3D SSFP axial scan encompassing the whole heart, was obtained to serve as a 3D localizer. The data were acquired in mid-diastole (12) and at end-expiration. The sequence parameters were as follows: in-plane resolution 2.1 × 2.1 mm^2, slice thickness 6 mm reconstructed to 3 mm using zero-filling interpolation, TR = 4.2 ms, TE 2.1 ms.

Coronary artery localization

From this second scout images, slice targeted double-oblique imaging planes along the major axes of the native left and right coronary system were prescribed using a previously described 3-point planscan tool (14). Three-dimensional high-resolution data were acquired for the left coronary artery system (LCA) and/or the RCA. Each slice-targeted 3D acquisition was performed in a separate scan. For LCA-plane definition, one point on the left main coronary artery, one on the proximal LCX and one on the LAD were identified on images of the second scout scan per interactive mouse click. For RCA, points near the ostium, mid-RCA and distal RCA were used for scan plane localization. The order of the left and right coronary artery system scan was performed in a randomized order.

Imaging sequence for cardiovascular magnetic resonance angiography

Double oblique navigator-gated (5 mm gating window) and corrected 3D SSFP CMRA with a T2 preparation (TE = 50 ms) and a spectrally selective fat saturation pre-pulse for endogenous contrast enhancement were obtained using the following sequence parameters: TR = 5.8–6.2 ms, TE 2.9–3.1 ms, flip angle = 110°, slice thickness 3 mm, 256 matrix, FOV 27 × 27 cm, 10 slices). During reconstruction, data were interpolated to a 512 × 512 matrix while 20 1.5 mm thick slices were obtained using zero-filling. The temporal resolution was 120 ms.

Q1

Image analysis

The image analysis was performed along the entire visualized course of the coronary arteries using a previously described semiautomtic "soapbubble" reformatting and analysis tool (15). Author 1 has ∼4 years, author 2 has ∼2 years, and the corresponding author has ∼10 years experience in acquiring and analyzing coronary CMR data. Both authors 1 and 2 learned the various coronary CMR techniques under the guidance of the corresponding author as part of their cardiovascular CMR research training at different times. Subsequently author 1 and 2 independently reformatted all the coronary CMR images and analyzed them for coronary length, diameter and vessel sharpness. The SNR/CNR measurements on all images were performed by author 1 only. The visual scoring was performed by authors 1 and 2.

Length measurements

After transferring data to the "soapbubble" tool, 3 orthogonal sections of the data set were simultaneously displayed, and the user navigated interactively through the entire data set. The RCA, LAD and LCX were visually identified in all 3 displayed planes. The 3D pathway of the coronary was then multiplanar reformatted, and the true visible lengths of individual segments of the native coronary arteries (RCA, LCX and LAD including the left main) were semi-automatically assessed in the reformatted images by author 1 and author 2 (15).

Vessel sharpness and diameter measurements

Along the path defined by the user-identified points used for length measurement, vessel sharpness and diameter measurements were made independently by authors 1 and 2. Hereby, and as earlier described by Botnar et al. (3), the local image gradient was obtained utilizing a full-width-half-maximum criterion in conjunction with a Deriche algorithm (16). Vessel sharpness and vessel diameter (mm) of the user specified segments of RCA and LCA were then automatically measured perpendicular to first 4 cm of each coronary artery in equidistant steps of 0.2 mm. The quantitative values along this coronary segment were averaged and stored electronically in an ASCII file.

Signal-to-noise/Contrast-to-noise

In all volunteers, regions of interest (ROIs) were defined (by author 1) in areas of myocardium, the intra-aortic blood-pool close to coronary ostia, and in a region anterior to the chest wall, where no respiration-induced motion artifacts were visually identified. Signal-to-noise (SNR) was defined as the mean signal intensity found in the blood-pool divided by the standard deviation found in the ROI anterior to the chest wall (17) (Equation 1). SNR was evaluated using the following formula:

$$\mathrm{SNR} = \frac{S_{\mathrm{Mean,Blood}}}{\mathrm{SDEV}_{\mathrm{Background}}}, \qquad [1]$$

Table 1. Image Quality Assessment (adopted from McConnell et al. [18])

Score	Grading	Description
1	Poor	Coronary artery visible with markedly blurred borders/ edges
2	Good	Coronary artery visible with moderately blurred borders/ edges
3	Very good	Coronary artery visible with mildly blurred borders/ edges
4	Excellent	Coronary artery visible with sharpley defined borders/ edges

where $S_{\mathrm{Mean,Blood}}$ denotes the mean signal intensity in the user defined region and $\mathrm{SDEV}_{\mathrm{Background}}$ relates to the standard deviation of the mean of the signal intensity anterior to the chest.

SNR of the muscle signal was determined in the muscle of the LV anterolateral wall at the level of proximal RCA.

Contrast-to-noise ratio (CNR) was defined as the difference of the mean signal intensities in two user specified ROIs divided by the standard deviation found in the ROI anterior to the chest wall (17) (Equation 2). The CNR between blood and muscle was defined as:

$$\mathrm{CNR} = \frac{S_{\mathrm{Mean,Blood}} - S_{\mathrm{Mean,Muscle}}}{\mathrm{SDEV}_{\mathrm{Background}}}. \qquad [2]$$

Visual scoring of the quality of angiograms

Subsequently, a consensus reading was performed for image quality scoring on all the angiograms in a blinded and random order by 2 readers (author 1 and author 2). Prior to beginning the analysis, authors 1 and 2 and the corresponding author had a conference discussing the rules for qualtitative assessment followed by a trial assessment of 5 separate CMR images for quality assurance. The method of qualitative assessment was adopted from McConnell et al. (18) and is described in Table 1.

Statistical analysis

Statistical analysis was performed by author 2 after extensive discussion with other co-authors. Continuous variables are reported as mean ± standard deviation. Paired t-testing was used to compare continuous variables (vessel length, vessel diameter, SNR, CNR, vessel sharpness and qualitative visual assessment) as appropriate. Reproducibility of coronary arterial luminal dimension was assessed by linear regression, Bland-Altman analysis (19) and intra-class correlation coefficients (ICC) (20, 21). Two readers (1st and 2nd authors) measured LAD, LCX and RCA luminal diameters on all (original and repeat) scans (inter-observer assessment). Subsequently, reader 1 (1st author) repeated the same measurements on the same scan in a random order about 1 week later in a blinded fashion (intra-observer assessment). For inter-scan measurements, the diameter measurements from author 1 was included. Based on these, intra-observer (two measurements done by 1st author), inter-observer (authors 1 and 2 measurements) and inter-scan agreement (original vs. repeat author 1 measurements) were assessed using Pearson's correlation coefficient, Bland-Altman technique and intraclass correlation coefficients (ICC). The following formula was used to generate ICC's:

$$ICC = \frac{(V_{Measurement1} + V_{Measurement2}) - (V_{Measurement1} - V_{Measurement2})}{(V_{Measurement1} + V_{Measurement2}) + (Mean_{Measurement1} - Mean_{Measurement2})^2 - \left(\frac{V_{Measurement1} - V_{Measurement2}}{n}\right)} \quad [3]$$

where V denotes variance and n denotes the total number of measurements.

Generalized estimating equations (GEE) were used to adjust standard errors for the clustering of 2 observations (left and right coronary arterial diameters) within the same individual (22). A p value < 0.05 was considered statistically significant.

RESULTS

There were no complications during the study. The average heart rate was 65 beats per minute (maximal heart rate 90 beats per minute), with an average navigator efficency of 50%. The time of imaging for each vessel was 4–6 minutes. The average total time for completing CMRA data collection in each volunteer was 25–30 minutes. Because of scheduling constraints that were not identical at both participating centers, not all individuals underwent scanning of all coronary arteries. This limitation is the reason for the discrepancy in the number of right and left coronary systems scanned.

Coronary vessel length

The mean measured length of RCA (12.5 ± 2.2 vs. 12.4 ± 2.4 cm), LAD (8.0 ± 2.0 vs. 8.0 ± 1.2 cm) and LCX (4.8 ± 2.2 cm vs. 4.6 ± 2.2 cm) imaged for original and repeat scans were not significantly different (all $p > 0.30$). However, the mean measured length of imaged RCA was significantly higher than that of the LAD and the LCX (both $p < 0.001$). The mean measured length of imaged LAD was also significantly higher than that of the LCX ($p < 0.001$).

Luminal Diameter

The mean luminal diameter of 1st 4 cm of the RCA (2.5 mm ± 0.4 vs. 2.6 mm ± 0.4), LAD (2.4 mm ± 0.3 vs. 2.4 mm ± 0.4) and LCX (2.0 mm ± 0.2 vs. 2 mm ± 0.3 mm) imaged for original and repeat scans were not significantly different (all $p > 0.20$). The mean diameter of female volunteers was smaller compared to male volunteers (RCA: 2.3 cm ± 0.3 vs. 2.7 cm ± 0.3 and LCA 2.3 cm ± 0.2 vs. 2.5 cm ± 0.2).

Results of inter-and intra-observer as well as inter-scan reproducibility were compared using Linear Regression (LG), Intra-class Correlation Coefficient (ICC) and Generalized Estimating Equations (GEE) and are summarized in Table 2.

Results of agreements on Bland-Altman analysis are shown in Figs. 3, 4 and 5.

Vessel Wall Sharpness

The mean vessel sharpness for RCA (42% ± 5 vs. 43% ± 8, $p = 0.57$), LAD (46% ± 17 vs. 46% ± 14, $p = 0.98$) and LCX (40% ± 4 vs. 42% ± 6, $p = 0.25$) were not significantly different between the original and repeat scans. There was no significant difference in vessel sharpness between RCA, LAD and LCX.

SNR and CNR

Mean ROI areas (in pixel) for the RCA were as follows: Blood (349 ± 413), background (1553 ± 1308) and muscle (140 ± 292). Similarly, the mean ROI sizes for the LCA were as follows: blood (480 ± 232), background (1530 ± 1588) and muscle (228 ± 240). Mean SNR was similar between original and repeat scans for both RCA (54 ± 13 vs. 51 ± 18, $p = 0.21$) and LCA (42 ± 13 vs. 40 ± 13, $p = 0.54$). The mean SNR of the RCA was significantly higher than that of LCA ($p < 0.001$ for both original and repeat scans). Mean CNR was similar between original and repeat scans for both RCA (39 ± 10 vs. 35 ± 13, $p = 0.28$) and LCA (25 ± 8 vs. 24 ± 11, $p = 0.98$). The mean CNR of the RCA was significantly higher than that of the LCA ($p < 0.001$ for both original and repeat scans).

Qualitative assessment

The mean qualitative visual scores were similar for initial and repeat scans for all 3 arteries: RCA (2.9 ± 0.9 vs 2.9 ± 1.2,

Table 2. The mean luminal diameter of the first 4 cm of the right (RCA), left (LCA) and left circumflex coronary artery (LCX) of the user specified segments were automatically measured using the "Soap-Bubble" Software (15). Two independent readers measured inter-observer, intra-observer and inter-scan reproducibility. Results were compared using Linear Regression (LG), Intra-class Correlation Coefficient (ICC) and Generalized Estimating Equations (GEE)

Reproducibility	RCA			LAD			LCX		
	LR*	ICC	GEE*	LR*	ICC	GEE*	LR*	ICC	GEE*
Intra-observer	0.99	0.98	0.988	0.90	0.89	0.898	0.85	0.95	0.850
Inter-observer	0.98	0.98	0.991	0.90	0.89	0.899	0.88	0.94	0.871
Inter-scan	0.84	0.86	0.988	0.81	0.63	0.724	0.81	0.79	0.794

*$p < 0.001$.

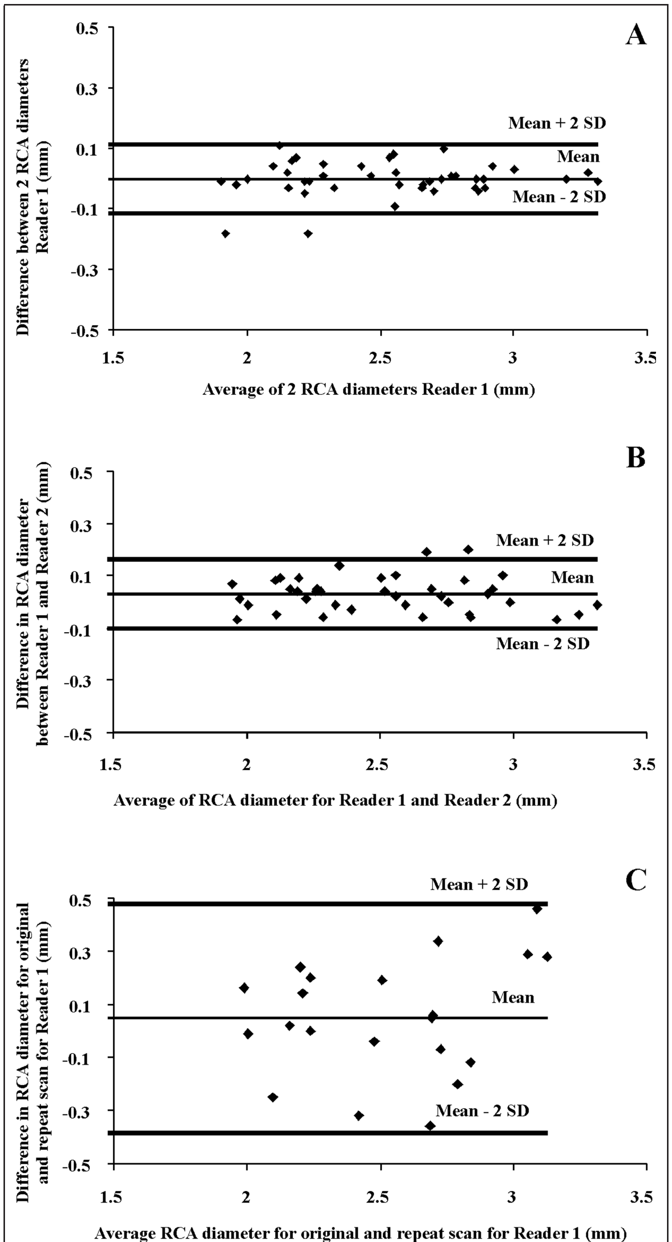

Figure 3. Graphs showing agreement in the mean diameter (mm) of the first 4 cm of the right corornay artery (RCA) using the Bland-Altman technique: (**a**) intra-observer (2 reader 1 measurements) agreement, (**b**) inter-observer (reader 1 vs. reader 2 measurement) agreement and (**c**) inter-scan (original vs. repeat scan measurements for reader 1) agreement.

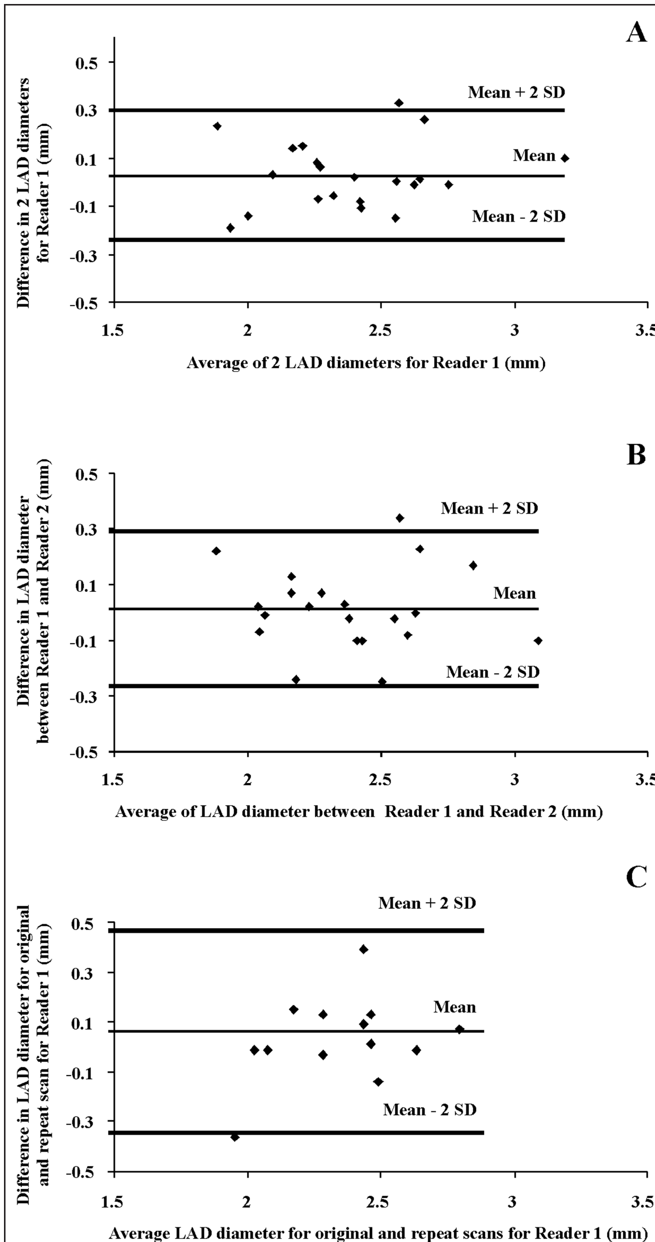

Figure 4. Graphs showing agreement in the mean diameter (mm) of the first 4 cm of the left anterior descending artery (LAD) using the Bland-Altman technique: (**a**) intra-observer (2 reader 1 measurements) agreement, (**b**) inter-observer (reader 1 vs. reader 2 measurement) agreement and (**c**) inter-scan (original vs. repeat scan measurements for reader 1) agreement.

$p = 1.0$), LAD (2.6 ± 0.9 vs. 2.4 ± 1.1, $p = 0.63$) and LCX (2.2 ± 0.9 vs. 2.0 ± 1, $p = 0.49$). However, mean visual score for the LCX was significantly lower than that from the LAD and RCA ($p = 0.04$ and 0.02, respectively). There was no significant difference in the visual score between the 2 centers.

DISCUSSION

This 2 center study demonstrates that CMRA using a 3D free-breathing SSFP sequence is a highly feasible technique for qualitative and some quantitative assessment of all 3 major epicardial coronary arteries. Using this technique, we were able to consistently image long contiguous segments of each coronary artery. The mean vessel length and diameter imaged by our technique was similar to what has been published in literature, for all 3 coronary arteries (23–26). This study further demonstrates that the mean imaged length, SNR, CNR and vessel sharpness of RCA, LAD and LCX were similar for original and repeat scans. Using a semi-automatic analysis tool (13, 15),

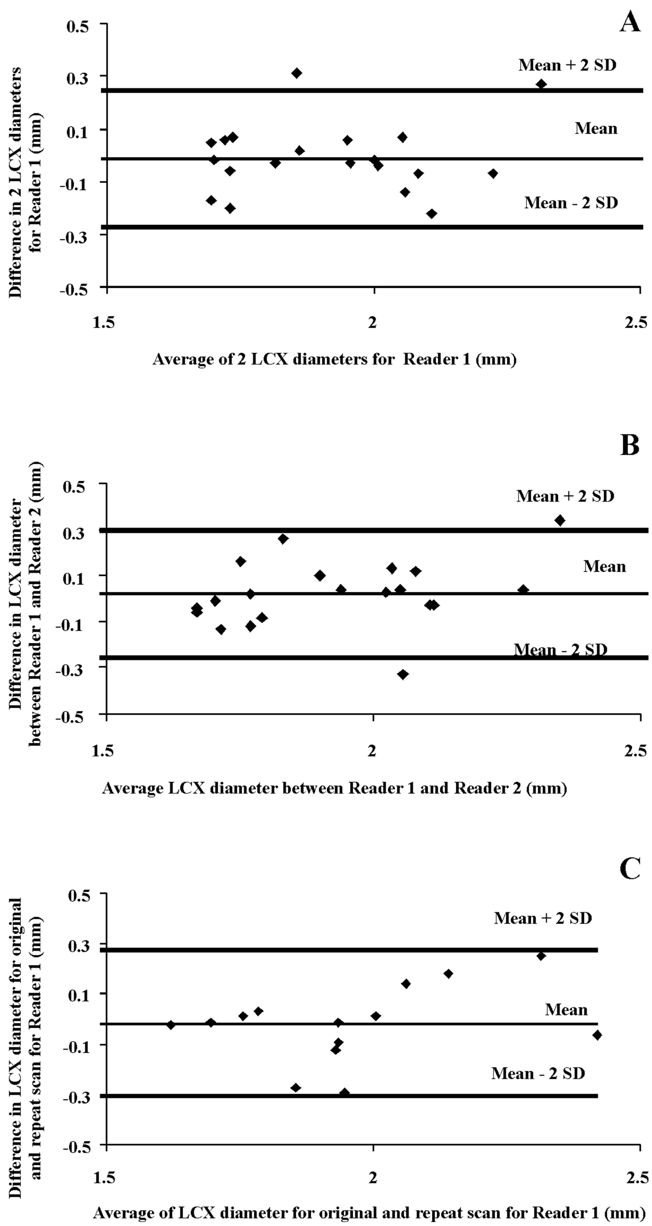

Figure 5. Graphs showing agreement in the mean diameter (mm) of the first 4 cm of the left circumflex (LCX) artery using the Bland-Altman technique: (**a**) intra-observer (2 reader 1 measurements) agreement, (**b**) inter-observer (reader 1 vs. reader 2 measurement) agreement and (**c**) inter-scan (original vs. repeat scan measurements for reader 1) agreement.

a high degree of intra-observer, inter-observer and inter-scan agreement in coronary artery dimension measurements of the RCA, LAD and LCX averaged over the proximal 4 cm of each coronary artery was also demonstrated. A recently published study also examined the reproducibility of CMRA at a single center (27). However, unlike our study, only the axial dimension of a particular coronary artery at 1 level was measured. Furthermore, the reproducibility was not based upon the arterial tree (right vs. left) and did not use the 3D free-breathing technology that has been successfully used in a multicenter trial (2).

Our data also suggest that measured artery length, CNR, SNR, and qualitative image quality assessment were significantly higher for the RCA as compared to the LAD or LCX. Lower SNR and CNR values for the LCA as compared to the RCA may be explained by increased distance from the surface coils and the scan plane localization. Although there was a high degree of agreement in the measured diameter of the first 4 cm of RCA, LCX and LAD, the technique appears to have better results for imaging the RCA. These results are also apparent by visual assessment. Finally, a consensus visual score on the image quality was applied, and consistent with numerical findings, it demonstrated that the average image quality of the RCA was significantly better than that of both LAD and LCX, most likely due to closer proximity of the RCA to the surface coils. This is consistent with the findings of an earlier multi-center trial (2).

This study has the following potential limitations. Increased heart rates (up to 90 beats per minute in some of our volunteers) adversely affect image quality. It is important to notice that the vast majority of patients with CAD are treated with beta-blockers clinically, reducing the heart rate to ~ 60 beats per minute. Such a reduced heart rate will support improved image quality in SSFP CMRA.

Each coronary arterial system was planned separately for this volume-targeted approach. More distal parts particulary of the LAD or LCX may not be easily imaged due to insufficient volumetric coverage. Even though the 3 point planscan tool facilitates co-registration between original and repeat scans, there might be slight differences in slice planning. Reduced length and lower reproducibility for the LCA compared to the RCA may be partially related to the above problem. The recently proposed whole heart approach (28) may help to overcome these limitations, but prolonged scan times, and longer acquisition windows have to be considered.

Because of scheduling constraints that were not identical at both participating centers, not all individuals underwent scanning of all coronary arteries. This is a limitation and the reason for the discrepancy in the number of right and left coronary systems scanned. This study included volunteers with no known CAD. Whether these results can be extrapolated to patients with atherosclerosis and CAD remains to be investigated. However, the high degree of reproducibility and the fact that the images were independently obtained and analyzed at two centers by different operators underscores the level of maturity of this technique, the semiautomatic analysis software, and potential readiness to be employed in longitudinal studies involving patients with known CAD.

Three-dimensional free-breathing CMR appears to be a highly reproducible technique for assessment of coronary artery dimensions. Using higher magnetic field strengths to improve spatial resolution (by trading in some of the SNR) (29), reducing scanning time by employing faster sequences and parallel imaging techniques like sensitivity encoding (30,31), improving coverage by use of whole heart approach (28), and the use of newer intravascular contrast agents to improve SNR

(9–11) may help to overcome some of its residual technical limitations.

CONCLUSIONS

Free-breathing 3D SSFP CMRA is a rapid, non-invasive technique which can repeatedly visualize long coronary arterial segments, with high reproducibility. Imaging of the LCA is technically more challenging than RCA as demonstrated by an average smaller length imaged, poorer SNR and CNR, and slightly reduced reproducibility. Also, in order to maintain and improve the inter-scan reproducibility for follow up studies, careful planning of the imaged volume position is necessary.

CMRA may have a potential role in following of development or progression of CAD in longitudinal therapeutic studies. However, further studies in patients with CAD are needed.

REFERENCES

1. Michaud CM, Murray CJ, Bloom BR. Burden of disease–implications for future research. JAMA 2001;285:535–9.
2. Kim WY, Danias PG, Stuber M, et al. Coronary magnetic resonance angiography for the detection of coronary stenoses. N Engl J Med 2001;345:1863–9.
3. Botnar RM, Stuber M, Danias PG, Kissinger KV, Manning WJ. Improved coronary artery definition with T2-weighted, free-breathing, three-dimensional coronary MRA. Circulation 1999;99:3139–48.
4. Spuentrup E, Katoh M, Buecker A, et al. Free-breathing 3D steady-state free precession coronary MR angiography with radial k-space sampling: comparison with cartesian k-space sampling and cartesian gradient-echo coronary MR angiography–pilot study. Radiology 2004;231:581–6.
5. Danias PG, Stuber M, Botnar RM, et al. Coronary MR angiography clinical applications and potential for imaging coronary artery disease. Magn Reson Imaging Clin N Am 2003;11:81–99.
6. Edelman RR, Manning WJ, Burstein D, Paulin S. Coronary arteries: breath-hold MR angiography. Radiology 1991;181:641–3.
7. Brittain JH, Hu BS, Wright GA, Meyer CH, Macovski A, Nishimura DG. Coronary angiography with magnetization-prepared T2 contrast. Magn Reson Med 1995;33:689–96.
8. Deshpande VS, Shea SM, Laub G, Simonetti OP, Finn JP, Li D. 3D magnetization-prepared true-FISP: a new technique for imaging coronary arteries. Magn Reson Med 2001;46:494–502.
9. Huber ME, Paetsch I, Schnackenburg B, et al. Performance of a new gadolinium-based intravascular contrast agent in free-breathing inversion-recovery 3D coronary MRA. Magn Reson Med 2003;49:115–21.
10. Herborn CU, Schmidt M, Bruder O, Nagel E, Shamsi K, Barkhausen J. MR coronary angiography with SH L 643 A: initial experience in patients with coronary artery disease. Radiology 2004;233:567–73.
11. Paetsch I, Huber ME, Bornstedt A, et al. Improved three-dimensional free-breathing coronary magnetic resonance angiography using gadocoletic acid (B-22956) for intravascular contrast enhancement. J Magn Reson Imaging 2004;20:288–93.
12. Stuber M, Botnar RM, Danias PG, Kissinger KV, Manning WJ. Submillimeter three-dimensional coronary MR angiography with real-time navigator correction: comparison of navigator locations. Radiology 1999;212:579–87.
13. Fischer SE, Wickline SA, Lorenz CH. Novel real-time R-wave detection algorithm based on the vectorcardiogram for accurate gated magnetic resonance acquisitions. Magn Reson Med 1999;42:361–70.
14. Stuber M, Botnar RM, Danias PG, et al. Double-oblique free-breathing high resolution three-dimensional coronary magnetic resonance angiography. J Am Coll Cardiol 1999;34:524–31.
15. Etienne A, Botnar RM, Van Muiswinkel AM, Boesiger P, Manning WJ, Stuber M. “Soap-Bubble” visualization and quantitative analysis of 3D coronary magnetic resonance angiograms. Magn Reson Med 2002;48:658–66.
16. Deriche R. Fast algorithms for low-level vision. IEEE Transactions on Pattern Analysis and Machine Intelligence 1990;12:78–87.
17. Arai AE, Epstein FH, Bove KE, Wolff SD. Visualization of aortic valve leaflets using black blood CMRI. J Magn Reson Imaging 1999;10:771–7.
18. McConnell MV, Khasgiwala VC, Savord BJ, et al. Comparison of respiratory suppression methods and navigator locations for MR coronary angiography. Am J Roentgenol 1997;168:1369–75.
19. Bland JM, Altman DG. Statistical methods for assessing agreement between two methods of clinical measurement. Lancet 1986;1:307–10.
20. Bartko JJ. The intraclass correlation coefficient as a measure of reliability. Psychol Rep 1966;19:3–11.
21. Deyo RA, Diehr P, Patrick DL. Reproducibility and responsiveness of health status measures. Statistics and strategies for evaluation. Control Clin Trials 1991;12:142S–58S.
22. Zeger SL, Liang KY, Albert PS. Models for longitudinal data: a generalized estimating equation approach. Biometrics 1988;44:1049–60.
23. Pennell DJ, Keegan J, Firmin DN, Gatehouse PD, Underwood SR, Longmore DB. Magnetic resonance imaging of coronary arteries: technique and preliminary results. Br Heart J 1993;70:315–26.
24. Manning WJ, Li W, Boyle NG, Edelman RR. Fat-suppressed breath-hold magnetic resonance coronary angiography. Circulation 1993;87:94–104.
25. Paschal CB, Haacke EM, Adler LP. Three-dimensional MR imaging of the coronary arteries: preliminary clinical experience. J Magn Reson Imaging 1993;3:491–500.
26. Botnar RM, Stuber M, Danias PG, Kissinger KV, Bornert P, Manning WJ. Coronary magnetic resonance angiography. Cardiol Rev 2001;9:77–87.
27. Keegan J, Horkaew P, Buchanan TJ, Smart TS, Yang GZ, Firmin DN. Intra- and interstudy reproducibility of coronary artery diameter measurements in magnetic resonance coronary angiography. J Magn Reson Imaging 2004;20:160–6.
28. Weber OM, Martin AJ, Higgins CB. Whole-heart steady-state free precession coronary artery magnetic resonance angiography. Magn Reson Med 2003;50:1223–8.
29. Stuber M, Botnar RM, Fischer SE, et al. Preliminary report on in vivo coronary MRA at 3 Tesla in humans. Magn Reson Med 2002;48:425–9.
30. Kozerke S, Tsao J. Reduced data acquisition methods in cardiac imaging. Top Magn Reson Imaging 2004;15:161–8.
31. Pruessmann KP, Weiger M, Scheidegger MB, Boesiger P. SENSE: sensitivity encoding for fast CMRI. Magn Reson Med 1999;42:952–62.